Journal of Histochemistry & Cytochemistry 2019, Vol. 67(8) 601–611

DOI: 10.1369/0022155419847188
journals.sagepub.com/home/jhc
SAGE

The Role of IFT140 in Osteogenesis of Adult Mice Long Bone

Dike Tao, Hui Xue, Chenyang Zhang, Gongchen Li, and Yao Sun
Department of Implantology, School & Hospital of Stomatology, Tongji University, Shanghai Engineering Research Center of Tooth Restoration and Regeneration, Shanghai, China (DT, HX, CZ, GL, YS)

Summary
Primary cilia have a pivotal role in bone development and the dysfunctions of primary cilia cause skeletal ciliopathies. Intraflagellar transport (IFT) proteins are conserved mediators of cilium signaling. IFT sub-complex A is known to regulate retrograde IFT in the cilium. As a core protein of IFT complex A, IFT140 has been shown to have a relationship with serious skeletal ciliopathies caused in humans. However, the effects and mechanisms of IFT140 in bone formation have not been systematically disclosed. To further investigate the potential role of IFT140 in osteogenesis, we established a mouse model by conditional deletion of IFT140 in pre-osteoblasts. The adult knock-out mice exhibited dwarf phenotypes, such as short bone length, less bone mass, and decreased bone mineral apposition rate. In addition, by IFT140 deletion, the expressions of several osteoblastic markers were decreased and loss of bone became severe with aging. These results suggest that cilia gene Ift140 is essential in bone development. (J Histochem Cytochem 67: 601–611, 2019)

Keywords
bone formation, intraflagellar transport, primary cilium

Introduction

Protruding from cell surface, primary cilia act as an antenna in most eukaryotic cells.[1] Recent studies indicate that primary cilia play a pivotal role in development and functioning of multiple organs by mediating signaling transduction and mechanosensation.[2] The dysfunction of primary cilia will cause a series of diseases called ciliopathies.[3] The maintenance and signaling of cilia require large protein particles, intraflagellar transport (IFT) complex, which is the bidirectional movement signal transport complex driven by motors within the cilium. There are two IFT complexes in cilium: IFT complex B which transports signals from the basal body to the ciliary tip by kinesin-2 motor, while retrograde IFT transports inversely through dynein motor and IFT complex A.[4,5] The integrity of IFT-A is essential for cilia stability and proper cellular localization. IFT complex A consists of 6 subunits: IFT144, IFT140, IFT122, IFT139, IFT121, and IFT43.[6] Due to the regulation of ciliogenesis and retrograde transport, loss of IFT140, IFT144, or IFT121 could cause very short cilia or even loss of cilia entirely.[7–9] Mutations in IFT-A members could cause a set of related symptoms with multiple organ defects accompanied by skeletal anomalies.[10–12]

Bone is a highly mineralized tissue that undergoes continuous remodeling during embryonic development, homeostasis, and wound healing.[13] All dysfunctions of bone formation occurring during the development and remodeling will cause severe bone diseases. Recent researches indicate that primary cilia have an essential role in bone development, and there is a close connection between IFT mutations

Received for publication February 11, 2019; accepted April 1, 2019.

Corresponding Author:
Yao Sun, Department of Implantology, School & Hospital of Stomatology, Tongji University, Shanghai Engineering Research Center of Tooth Restoration and Regeneration, 399 Middle Yanchang Road, Shanghai 200072, China.
E-mail: yaosun@tongji.edu.cn

Journal of Histochemistry & Cytochemistry

and clinical skeletal features.[14,15] It's worth noting that, for members of IFT complex A, gene mutation always causes skeletal phenotypes.[16] Among them, the mutation of IFT140 has been newly identified in patients with severe skeletal disorders. These bone dysplasia disease include Mainzer–Saldino syndrome (MSS),[17] Jeune asphyxiating thoracic dystrophy (JATD),[18] or Opitz trigonocephaly C syndrome (OTCS)[19] which commonly lead to phalangeal cone-shaped epiphyses, mild abnormalities of the proximal femur, shortened ribs, and a narrow, bell-shaped chest. As a model of Jeune syndrome, the Ift140$^{cauli/cauli}$ mice with a recessive missense mutation in the Ift140 gene also exhibit several skeletal development defects.[7] All these evidences indicate that Ift140 has an essential role in skeleton development. However, the links between the IFT complex A and patients with ciliopathies have not been well explored. In addition, due to the mid-gestational lethality, available Ift140$^{cauli/cauli}$ model has limitations to study the role of IFT140 during bone development and remodeling.

In this study, we established mouse model with pre-osteoblast-specific deletion of IFT140 (Osx-Cre; Ift140$^{flox/flox}$) to investigate functions of IFT140 in osteogenesis. The knock-out mice exhibited bone dysplasia with defects in bone formation. The detailed data presented here will further reveal the effects of osteogenesis regulated by IFT molecules in primary cilia.

Materials and Methods

Mouse Models

To investigate the role of IFT140 in bone formation, we generated conditional deleted Ift140 (Ift140-cKO) in pre-osteoblasts by crossing Ift140$^{flox/flox}$ mouse (Fig. 1A–C) with Osx-Cre mice. Detailed information remained the same as described previously.[20] Animals were maintained in a specific pathogen-free (SPF) facility under a 12/12h day/night illumination cycle. The mice were euthanized by cervical dislocation after inhalation anesthesia. The Animal Welfare Committee of Tongji University approved all animal experimental protocols used in this study.

Micro–CT Analysis

All femurs dissected from eight 8-week-old and eight 6-month-old female Ift140 cKO mice and control littermates were fixed in 4% paraformaldehyde (PFA) for 48 hr. The femurs were subjected to analysis by micro–CT 50 (Scanco Medical, Zurich, Switzerland) at a scan resolution of a 10-μm slice increment with a voltage of 70 kV and a current of 200 μA. For quantifying trabecular bone parameters, 100 CT slices immediately proximal to the distal femoral growth plate were analyzed. The parameters of trabecular bone volume/total volume (BV/TV), trabecular number (Tb.N), trabecular thickness (Tb.Th), structure model index (SMI), connective density (Conn.D), and bone mineral density (BMD) were quantified according to the standard procedures.[21]

Histological Analyses

For histological analyses, femurs from eight female Ift140 cKO and eight control mice were decalcified in 10% EDTA (pH 7.4) at 4C for 1 month. During dehydration through a graded ethanol series, specimens were embedded in paraffin and cut into 5-μm-thick sections. For morphological evaluation, the sections were stained with hematoxylin and eosin (H&E) (Sangon Biotech, Shanghai, China). To evaluate the content of collagen and proteoglycan, the sections were stained with Masson (Nanjing Jiancheng Bioengineering Institute, Nanjing, China) and alcian (Beijing Solarbio Science & Technology Co., Ltd. Beijing, China). For immunohistochemistry staining, sections were deparaffinized with xylene and rehydrated in a descending series of ethanol concentrations. Antigen retrieval was performed using hyaluronidase, then sections were treated with 3% hydrogen peroxide and goat serum blocking. Primary antibodies used were as follows: anti-DMP1-C-8G10.3 (1:300; gifts from Dr. Chunlin Qin, TA&M University, College of Dentistry) and anti-Osteocalcin (1:100; Santa Cruz Biotechnology, Dallas, TX). A DAB detection kit (Maxim Biotechnology, Fuzhou, China) was used to do color development. For immunofluorescence staining, specimens were embedded in OCT and sectioned at an 8-μm thickness after being decalcified. The sections were incubated with anti-acetylated α-tubulin (1:1000; Sigma-Aldrich, St Louis, MO) and by Alexa Fluor 488 IgG (1:1000; Invitrogen, Carlsbad, CA). Anti-IFT140 (1:50; Proteintech, Wuhan, China), anti-type II collagen (1:200; Boster Biological Technology, Wuhan, China) or anti-Ostreix (1:300; Abcam, Cambridge, UK) at 4C overnight and by Alexa Fluor 546 IgG (1: 1000; Invitrogen) and phalloidin at room temperature for 1 hr (50 μM; Sigma-Aldrich). Sections were subsequently stained with DAPI (Sigma-Aldrich). And *Von Kossa* staining was performed using 1% silver nitrate and 3% sodium thiosulfate solution counterstaining by nuclear fast red. For double fluorochrome labeling, Alizarin red (20 mg/kg; Sigma-Aldrich) was first injected into 8-week-old mice by intraperitoneal injection, followed by injection of calcein (5 mg/kg; Sigma-Aldrich) 7 days later. Meanwhile, we performed Van Gieson (Beijing Solarbio Science & Technology Co., Ltd. Beijing, China) staining of corresponding sections used in double fluorochrome labeling to

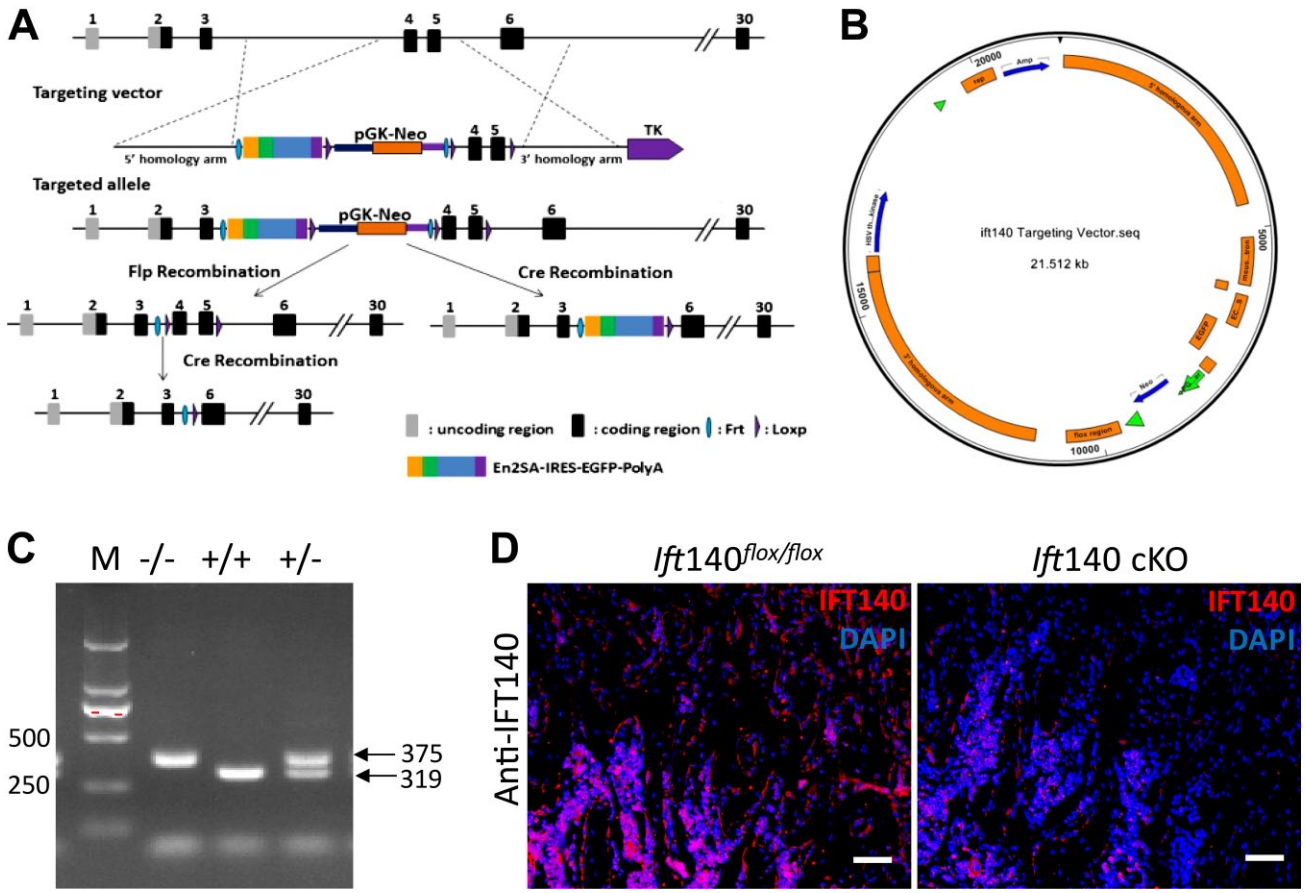

Figure 1. Deletion of IFT140 in pre-osteoblasts. (A) The design strategy of conditional deletion of Ift140 gene. (B) The targeting vector in embryonic stem (ES) cells based on C57BL/6J mice (Shanghai Biomodel Organism Science & Technology Development Co. Ltd, Shanghai, China). (C) Genotyping of $Ift140^{flox/flox}$ mice primers used for exons 4 and 5 conditional knock-out identification included the following: F-primer, 5'-ATCTTAATTTGTGTTGAAGGGGTT-3', and R-primer, 5'-CTGCCAGGGGTACATGGTAGTAAG-3'. Product size of endogenous Ift140 was 319 bp, and product size of $Ift140^{flox/flox}$ was 375 bp. (D) Immunofluorescence staining of IFT140 (red) in trabecular bone of 8-week-old mice. Ift140 cKO mice showed remarkably less expression of IFT140 in trabecular bone. Scale bars: 50μm.

display morphological image of bone cross section. The alkaline phosphatase (ALP) staining was performed using ALP assay kit and following the protocol (Sangon Biotech).

Quantitative RT-PCR Analysis

Total RNA was isolated from 2-mm bony segment under the growth plate of eight 8-week-old female Ift140 cKO and eight control mice by using Trizol reagent (Invitrogen) according to the manufacturer's protocol. cDNA was synthesized using a Transcriptor First Strand cDNA Synthesis Kit (Roche, Basel, Switzerland). A reaction mix was prepared using SYBR green master mix (Roche), following manufacturer instructions. The expression levels of target gene were evaluated by using Light Cycler 96 PCR system (Roche). Reactions of each sample needed to be run in triplicate. The primers used for osteogenic markers included the following: GAPDH-forward: 5'-TGTGT CCGTCGTGGATCTGA-3', GAPDH-reverse: 5'-CCTG CTTCACCACCTTCTTGA-3'; Alp-forward: 5'-GATCATT CCCACGTTTTCACATT-3', Alp-reverse: 5'-TTCACCGT CCACCACCTTGT-3'; Ocn-forward: 5'-GAGGACCATC TTTCTGCTCACTCT-3', Ocn-reverse: 5'-TTATTGCCC TCCTGCTTGGA-3'; Opn-forward: 5'-GATCAGGACAA CAACGGAAAGG-3', Opn-reverse: 5'-GCTGGCTTTGG AACTTGCTT-3'; Bsp-forward: 5'-AGGACTGCCGAAA GGAAGGTTA-3', Bsp-reverse: 5'-AGTAGCGTGGCC GGTACTTAAA-3'.

Statistical Analysis

All data were analyzed using Student's *t* test for two-group comparison by SPSS 20.0. The *p* values less than 0.05 were considered statistically significant.

Results

Deletion of IFT140 Stunted Bone Development in Mice

In order to investigate the role of IFT140 in bone formation, Osx-Cre; Ift140$^{flox/flox}$ mice were generated to specifically delete the Ift140 in pre-osteoblasts. First, we performed immunofluorescence staining of IFT140. There were significant fewer IFT140 positive cells in trabecular bone area of Ift140 cKO mice (Fig. 1D). As observed, 8-week-old Ift140 cKO mice exhibited growth retardation and smaller body size than that of control (Fig. 2A). And the body weight of Ift140 cKO mice was obviously decreased (Fig. 2B).

Less Bone Formation in 8-week-old Ift140 cKO Mice

Micro-CT scanning was employed to evaluate bone morphology and mass changes. Compared with controls, a narrow midshaft of bone marrow cavity, thinner trabecular bone, and cortical bone around trabecular bone were found in Ift140 cKO mice (Fig. 2C). The micro-CT analyses of trabecular bone indicated less bone mass in Ift140 cKO mice (Fig. 2D). Further histological analyses by H&E staining revealed less trabecular bone in ossification center of 8-week-old Ift140 cKO mice (Fig. 3A). Following merging of fluorochromes xylenol orange and calcein, the mineral deposition rate in the mid-shaft region of the femurs was compared. There was less bone deposition at the endocortical surface in Ift140 cKO mice at age 8 weeks (Fig. 3C and E). However, there was no obvious difference of Masson staining for matrix collagen between the Ift140 cKO mice and control littermates at age 8 weeks (Fig. 3B).

Reduced Expressions of Osteogenic Markers in Long Bone of Ift140 cKO Mice

To further identify the impaired bone formation and mineralization in Ift140 cKO mice, we then performed immunohistochemical analyses by using anti-DMP1 and anti-osteocalcin antibodies, and found that expression of DMP1 or osteocalcin was lower in Ift140 cKO bone (Fig. 4A). The ALP staining also showed that ALP activity in mutant osteoblasts was significantly decreased (Fig. 4B). The expression of Osterix also reduced in Ift140 cKO mice (Fig. 4C). And the mRNA expression levels of osteogenic markers (*Alp, Ocn, Opn, Bsp*) were all reduced in Ift140 cKO mice (Fig. 4D).

Lack of IFT140 Induced Severe Bone Loss With Aging

Ift140 cKO mice displayed a severe bone loss phenotype with aging. Micro-CT scanning showed intumescentia in metaphysis of femur, shortened femur length, and less trabecular bone in femurs of mutant mice (Fig. 5A). Due to loss of growth plate structure in aged Ift140 cKO mice (Fig. 5A and B), we didn't perform the bone histomorphometric analyses for secondary ossification center or trabecular bone area under growth plate. H&E and *Von Kossa* staining also exhibited significant bone loss (Fig. 5B). To further evaluate the quality of bone, Masson staining was performed and the results showed different collagen distributions and poor mineralization in cortical bone (Fig. 5D). Meanwhile, the expression levels of DMP1 and OCN were significantly reduced in Ift140 cKO mice by immunohistochemical analyses (Fig. 5E).

Phenotypes of Growth Plate in Ift140 cKO Mice

During the bone development and remodeling, we found another noteworthy phenotype of growth plate. At age 8 weeks, the chondrocytes of growth plate became abnormal in Ift140 cKO mice. The column arrangements of chondrocytes were disordered and replaced by mineralized bone tissue gradually (Fig. 6A and A'), which also resulted in decreased proteoglycans and hyaluronic acid in bone matrix according to alcian staining (Fig. 6B and B'). The expression level of type II collagen was also reduced in Ift140 cKO mice (Fig. 6C and C'). And to further investigate the turbulence of growth plate, we performed staining of IFT140 (Fig. 6D and D') and the axoneme to visualize primary cilia in chondrocytes (Fig. 6E and E'). The expression of IFT140 reduced in growth plate and there were fewer ciliated fluorescence positive cells in Ift140 cKO mice. Consequently, the growth plate began to disappear gradually and there was no growth plate at age of 6 months (Fig. 5B).

Discussion

IFT protein complex functions to transport various proteins within the cilia for participating transductions. Several IFT members have been proved to play key roles in regulating osteogenesis. Dysfunction of IFT molecules and primary cilia results in skeletal dysplasia.[22,23] IFT88, a member of IFT complex B, works in keeping cilia formation and function.[24] Deletion of Ift88 in Prx1-positive cells results stunted limb growth due to disruptions in endochondral and intramembranous ossification.[25] In

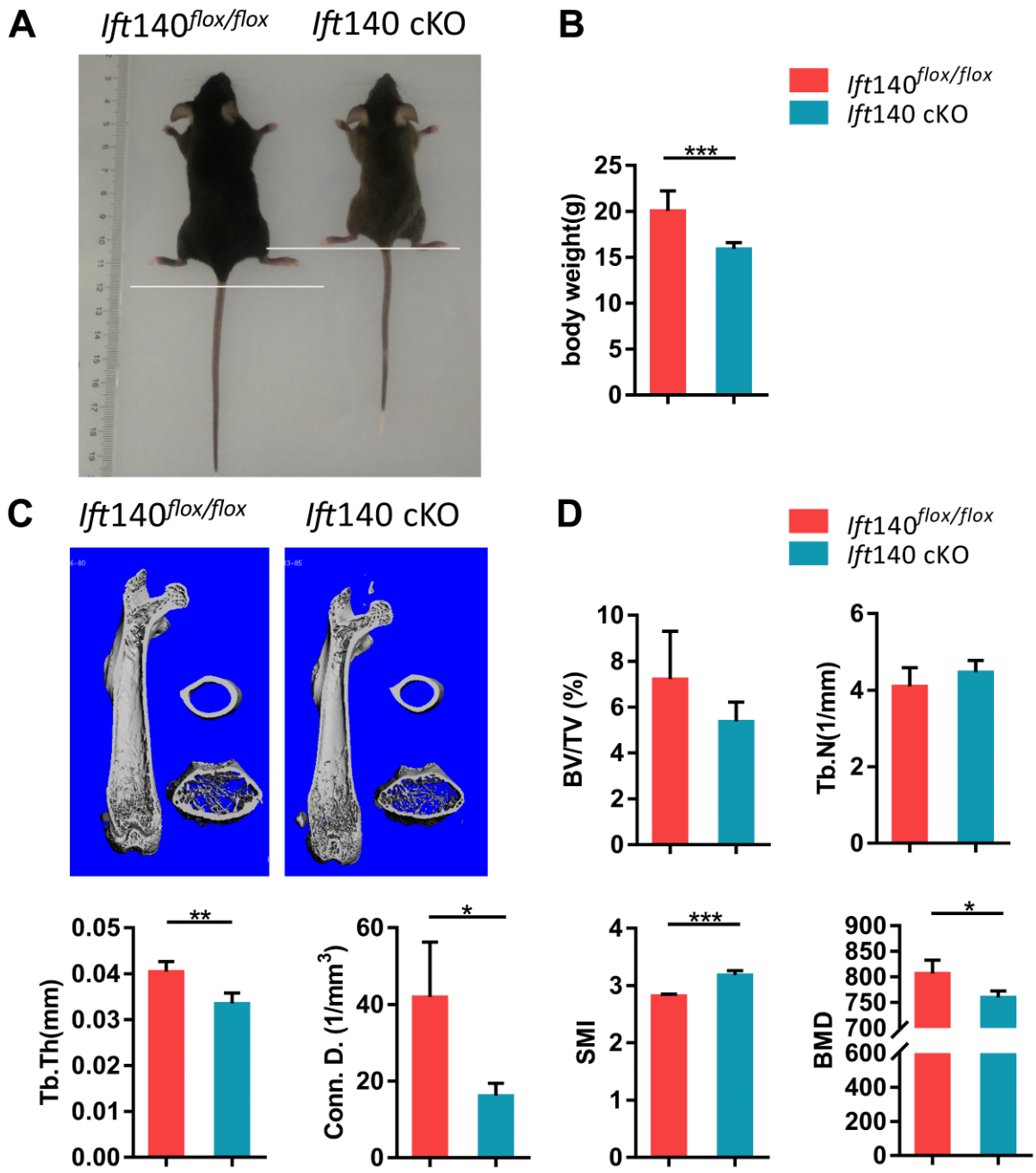

Figure 2. Bone phenotypes in Ift140 cKO mice. (A) Representative image of Ift140 cKO mice and control at 8-week-old. Body sizes of Ift140 cKO mice were shorter. (B) Quantification of body weight of Ift140 cKO mice and control at age 8 weeks, n=7. (C) Micro–CT analysis of femurs obtained from Ift140 cKO and control mice. Trabecular bones of IFT140 cKO mice were less and cortical bone of Ift140 cKO mice was thinner. (D) Quantitative micro-CT analysis of femur trabecular bone. *p<0.05, **p<0.01, ***p<0.001, n=5. Abbreviations: BV/TV, trabecular bone volume; CT, computed tomography; Tb.N, trabecular number; Tb.Th, trabecular thickness; Conn.D, connective density; SMI, structure model index; BMD, bone mineral density.

addition, deletion of Ift88 and subsequent depletion of primary cilia from chondrocytes (Col2a-Cre;Ift88$^{flox/flox}$) results in disorganized columnar structure and early loss of growth plate.[26] And deletion of Ift80, another IFT members, by using Osx-Cre also causes a significant growth retardation and osteopenia.[27] Similar to Ift88 and Ift80, loss of Ift140 also exhibited the impaired bone formation and growth retardation in mice. There were significant differences in body length and weight between Ift140 cKO mice and control mice at age 8 weeks. Meanwhile, in

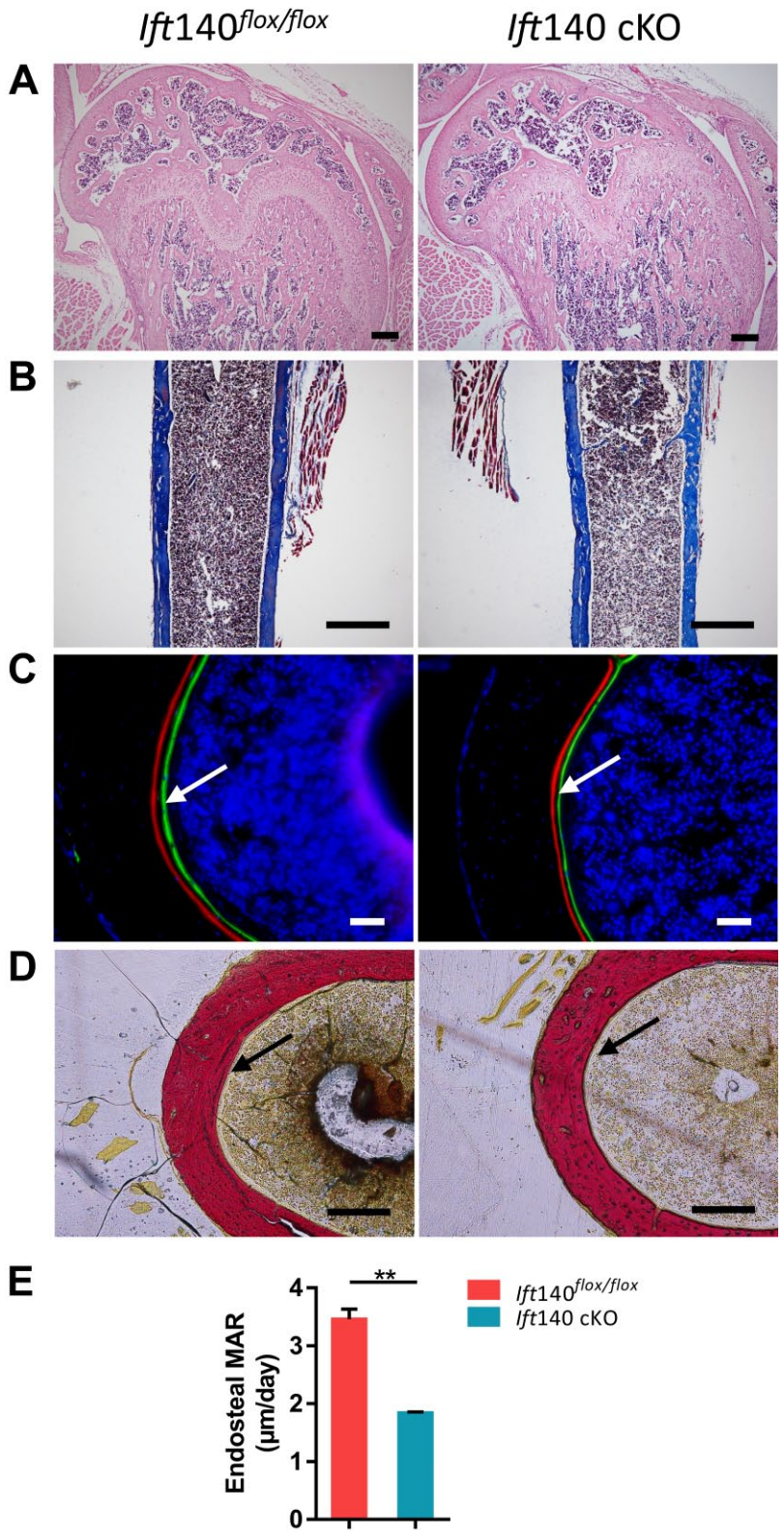

Figure 3. Reduced bone formation in Ift140 cKO mice at age 8 weeks. (A) Hematoxylin and eosin staining showed less and thinner trabecular bone in Ift140 cKO mice. Scale bars: 200 μm. (B) Masson staining showed no difference in collagen distribution in cortical bone. Scale bars: 100 μm. (C) Cross sections of femurs from control and Ift140 cKO mice. The distance between green (calcein) and red (Alizarin red) represented the mineral apposition rate of cortical bone in 7 d. The arrows showed the endocortical surface. Ift140 cKO mice had a slower mineral deposition rate compared with the control littermates. Scale bars: 50 μm. (D) Van Gieson staining of corresponding sections in 3C. The arrows showed the endocortical surface. Scale bars: 50 μm. (E) Quantitative measurements of the lower bone mineral apposition rate in Ift140 cKO mice. $^{**}p<0.01$, $n=4$.

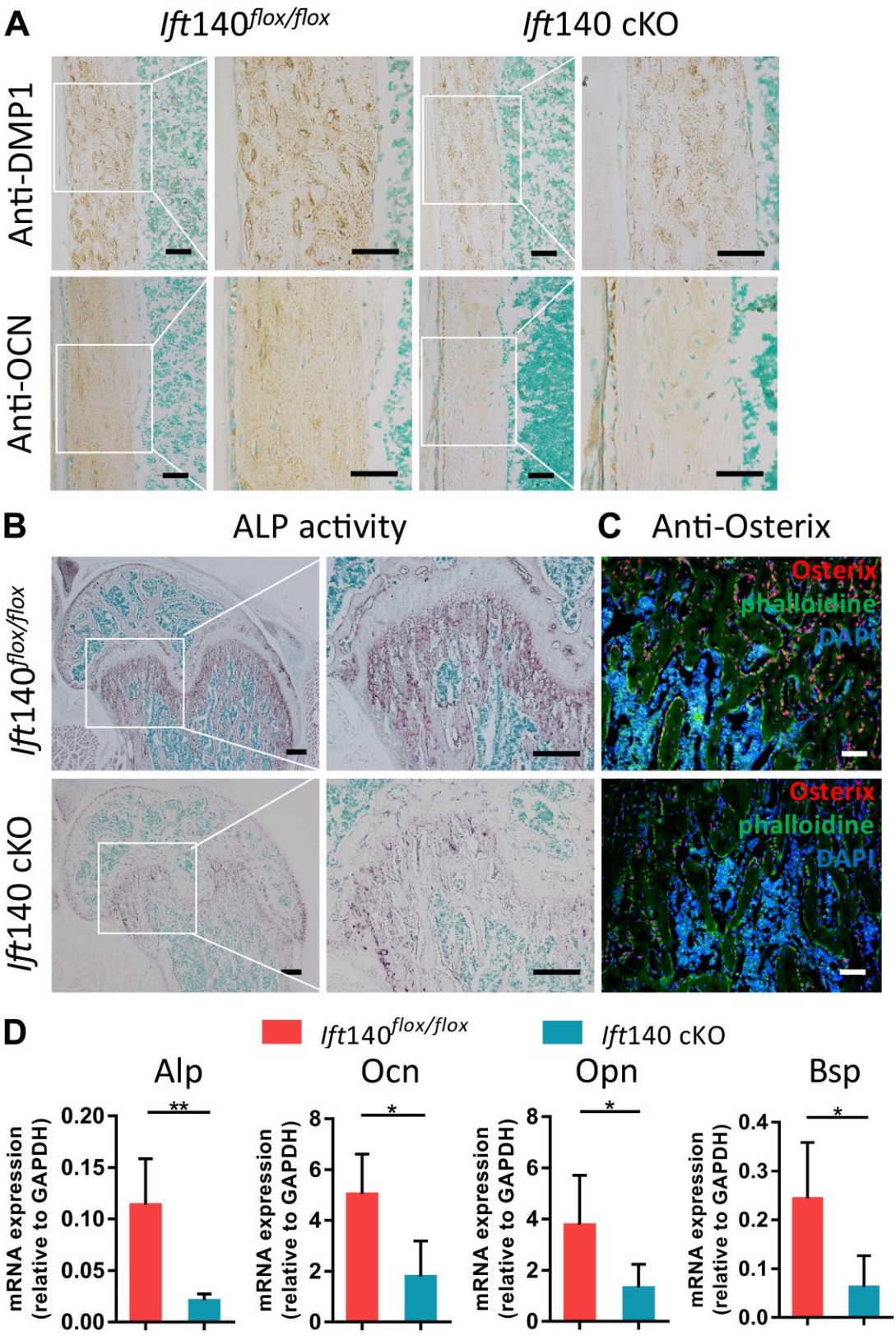

Figure 4. Disturbed osteogenic markers expressions in Ift140 cKO mice at age 8 weeks. (A) Immunohistochemistry (IHC) staining of DMP1 and OCN in cortical bone from 8-week-old mice. Ift140 cKO mice showed remarkably less expression of DMP1 and OCN in cortical bone matrix. Boxes in left panel were shown magnified in the right panel, respectively. Scale bars: 50 μm. (B) Alkaline phosphatase activity of trabecular bone. Ift140 cKO mice showed remarkably weakened staining. Boxes in up panel were shown magnified in the down panel, respectively. Scale bars: 200 μm. (C) Immunofluorescence staining of Osterix (red) in trabecular bone of 8-week-old mice. Ift140 cKO mice showed remarkably less expression of Osterix. Scale bars: 50 μm. (D) RT-qPCR quantification analysis of osteogenic markers. Ift140 cKO mice displayed down-regulated expression levels of *Alp, Ocn, Opn* and *Bsp*. *p<0.05, **p<0.01, n=5.

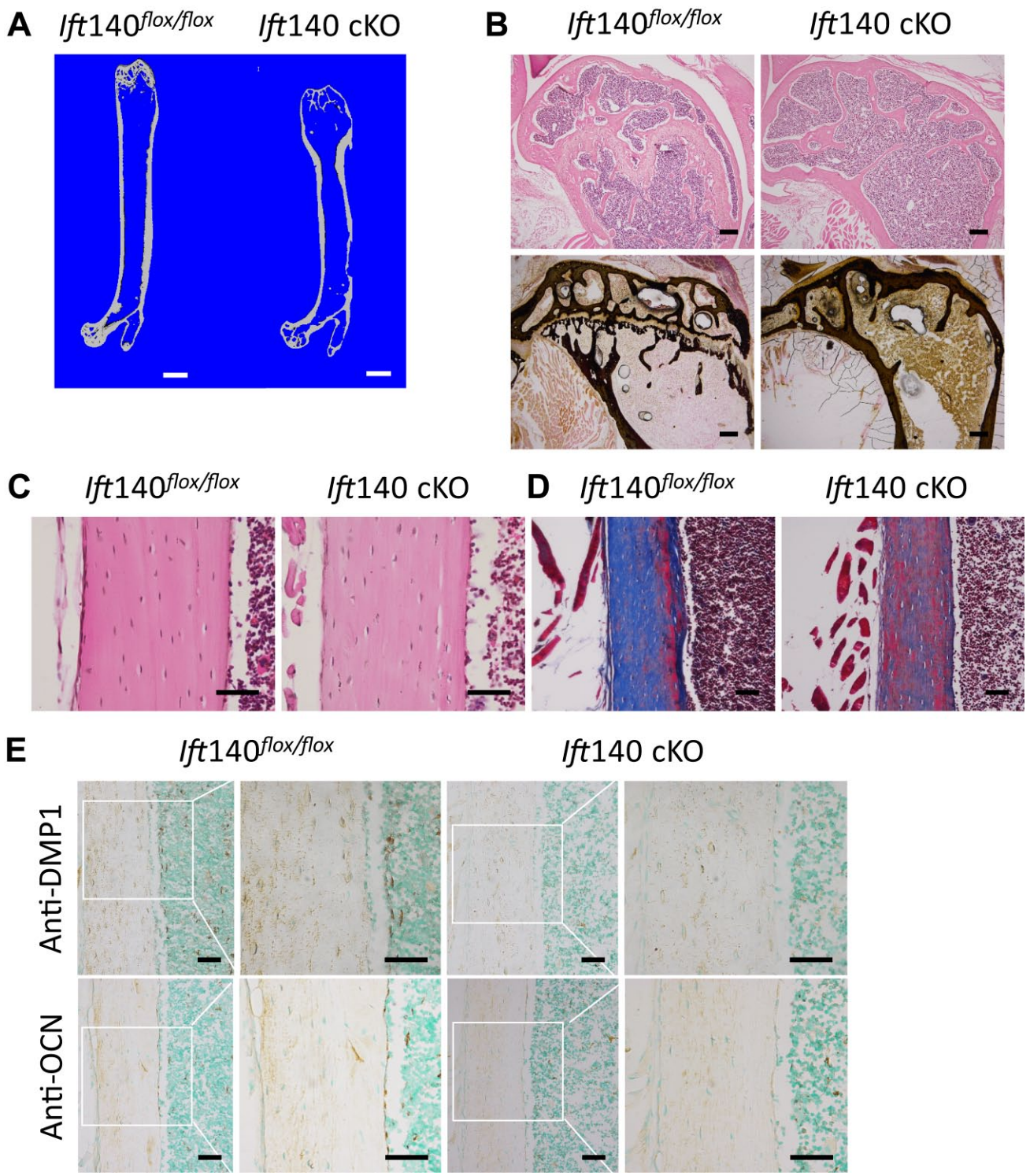

Figure 5. Severe bone abnormalities in Ift140 cKO mice at age 6 months. (A) Micro–computed tomography (CT) cross section scan of femur obtained from Ift140 cKO and control mice at age 6 months. Ift140 cKO mice showed severe morphological abnormality. Scale bars: 1 mm. (B) Hematoxylin and eosin staining and *Von Kossa* staining showed less trabecular bone and the disappearance of growth plate in 6-month-old Ift140 cKO mice. Scale bars: 200 μm. (C) Hematoxylin and eosin staining of cortical bone at age 6 months. Scale bars: 50 μm. (D) Masson staining of cortical bone exhibited abnormal collagen distributions and poor mineralization in Ift140 cKO mice at age 6 months. Scale bars: 50 μm. (E) Immunohistochemistry (IHC) staining of DMP1 and OCN of cortical bone from 6-month-old mice. Ift140 cKO mice showed remarkably less expression of DMP1 and OCN in cortical bone matrix. Boxes in left panel were shown magnified in the right panel, respectively. Scale bars: 50 μm.

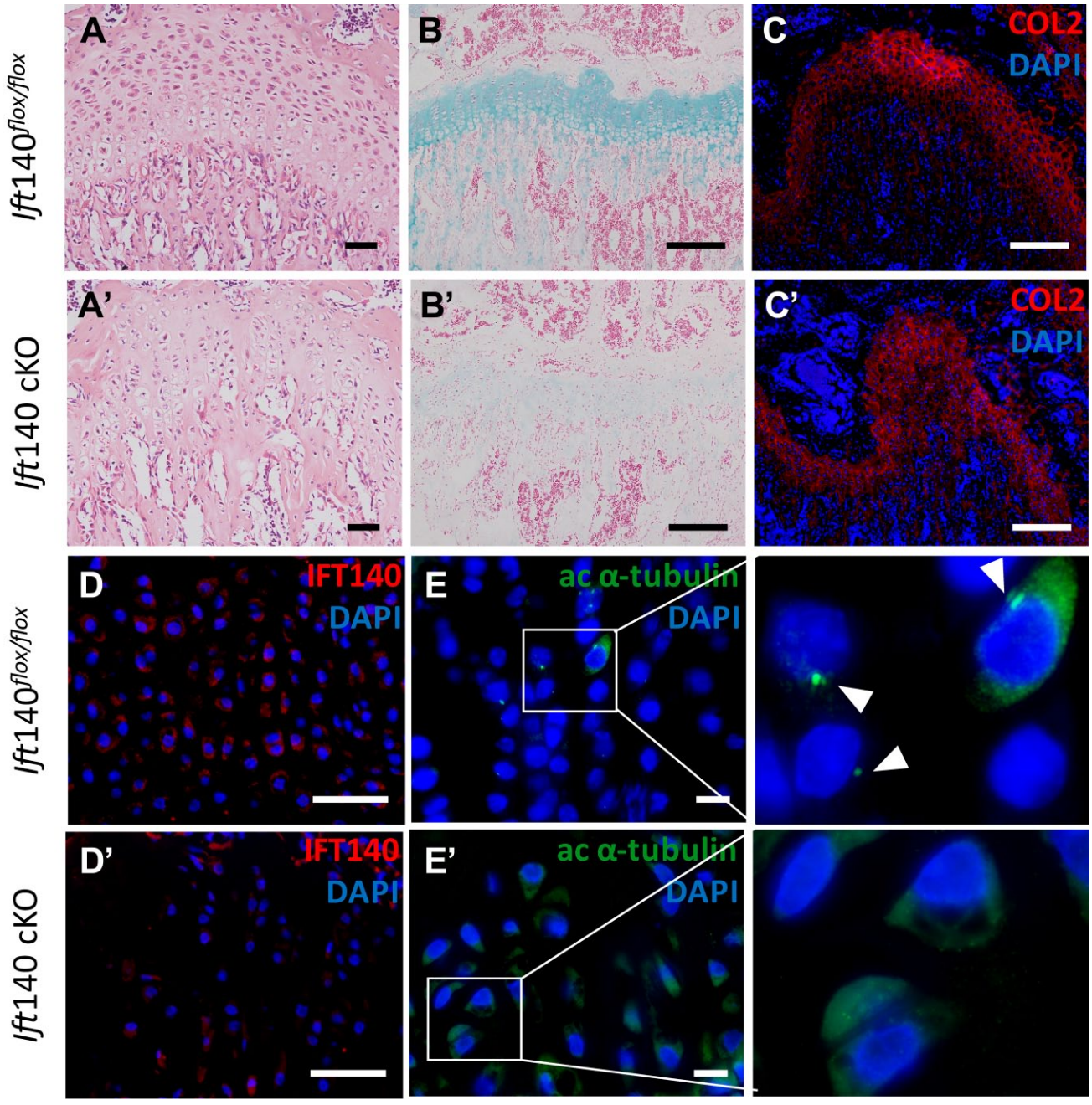

Figure 6. Defects of growth plate in Ift140 cKO mice. (A and A') Hematoxylin and eosin staining of growth plate showed disordered column arrangements in Ift140 cKO at age 8 weeks. Scale bars: 50 μm. (B and B') Alcian blue staining of growth plate at age 8 weeks. Scale bars: 200 μm. (C and C') Type II collagen (red) immunofluorescence staining in growth plate at age 8 weeks. Scale bars: 200 μm. (D and D') Immunofluorescence staining of IFT140 (red) in growth plate of 8-week-old mice. Ift140 cKO mice showed remarkably less expression of IFT140. Scale bars: 50 μm. (E and E') Immunofluorescence staining of acetylated α-tubulin (green) in cilia in growth plate of 8-week-old mice. Boxes in left panel were shown magnified in the right panel, respectively. Arrowheads showed the primary cilia. Scale bars: 50 μm.

Ift140 cKO mice, significant down-regulation of osteogenic markers began to be observed along with low mineral deposition rate. The osteodysplasia phenotypes of Ift140 cKO mice started at age 8 weeks and ultimately resulted in severe bone abnormalities at age 6 months. With aging, the Ift140 cKO mice displayed significant decrease in trabecular bone mass and mineralization in cortical bone. In addition, intumescent metaphysis area

in mouse long bone is consistent with phalangeal cone-shaped epiphyses in MSS, a human disease with Ift140 mutation.[28] And the abnormalities in metaphysis area are not reported in the phenotypes of other IFT gene knockout.

It is also interesting to know that, in the process of osteoblast differentiation, the role of IFT140 has time and space specificity. Osterix is a pre-mature osteoblast marker, and Osx-Cre could delete Ift140 in early stage during osteoblast maturation. By crossing $Ift140^{flox/flox}$ mice with Osx-Cre line, the descendants exhibit morphological abnormality in bone development and remodeling. In addition, by crossing $Ift140^{flox/flox}$ mice with Dmp1-cre mice, which targets the mature osteoblasts and osteocytes, the bone phenotypes are the same as that of wild-type mice (data not shown). According to this, we believe that the role of IFT140 in osteogenesis is mainly in the early stage of osteoblast differentiation.

Interestingly, we also noticed the abnormal phenotype on growth plate in our mouse model. Osx-Cre; $Ift140^{flox/flox}$ mice (Ift140 cKO mice) exhibited narrow and disorganized growth plate. Recent studies showed that primary cilia could also mediate chondrocyte rotation to maintain columnar organization.[6] In addition to osteoblasts, the Osx-Cre transgenic mice has been shown to direct Cre recombinase activity in pre-hypertrophic and hypertrophic chondrocytes in the growth plate.[29] The growth plate degeneration of Ift140 cKO mice began at age 8 weeks. The growth plate showed disorganized columnar structure of chondrocytes and ectopic osteogenesis. And it also exhibited lower expression level of type II collagen in Ift140 cKO mice. Consequently, the growth plate completely disappeared by conditional knock out Ift140 in 6-month-old mice. Due to the responsibility of growth plate in the longitudinal growth of bones,[30] the advanced degeneration of growth plate resulted in postnatal dwarfism phenotypes in Ift140 cKO mice. Our results also suggest that IFT140 could be required to maintain the growth plate by functioning in pre-hypertrophic and hypertrophic chondrocytes. And it still needs systematic investigation by using different stages of chondrocyte-specific Cre lines to explore the function of IFT140 in growth plate and chondrocytes.

In conclusion, our study provides information of IFT140 in regulating the skeleton development. And it indicates that IFT140 is essential for bone development by regulating the activity of pre-osteoblasts and also maintaining growth plate.

Acknowledgments

We gratefully acknowledge the DMP1-C antibody from Dr. Chunlin Qin (College of Dentistry, Texas A&M University). And we also appreciate Ruilin Zhang, Mengqi Zhou, and Qiqi Fan (Department of Implantology, School & Hospital of Stomatology, Tongji University) for their help in sample preparation.

Competing Interests

The author(s) declared no potential conflicts of interest with respect to the research, authorship, and/or publication of this article.

Author Contributions

All authors have contributed to this article as follows: DT for acquisition of data and drafting the article, HX for sample processing and statistical analysis, CZ and GL for revising article, and YS for design and manuscript reviewing.

Funding

The author(s) disclosed receipt of the following financial support for the research, authorship, and/or publication of this article: This study was founded by Key Project of Chinese National Programs for Research and Development (2016YFC1102705, Y. Sun), National Science Foundation of China (81822012, 81470715, and 81771043, Y. Sun), Shanghai Health System (2017 BR009, Y. Sun), and Basic scientific research operating expenses of central universities—Interdisciplinary research project of Tongji University (20173386).

Literature Cited

1. Delling M, Indzhykulian AA, Liu X, Li Y, Xie T, Corey DP, Clapham DE. Primary cilia are not calcium-responsive mechanosensors. Nature. 2016;531(7596):656–660.
2. Singla V, Reiter JF. The primary cilium as the cell's antenna: signaling at a sensory organelle. Science. 2006;313(5787):629–633.
3. Hildebrandt F, Benzing T, Katsanis N. Ciliopathies. N Engl J Med. 2011;364(16):1533–1543.
4. Satir P, Pedersen LB, Christensen ST. The primary cilium at a glance. J Cell Sci. 2010;123(Pt 4):499–503.
5. Rosenbaum JL, Witman GB. Intraflagellar transport. Nat Rev Mol Cell Biol. 2002;3(11):813–825.
6. Yuan X, Serra RA, Yang S. Function and regulation of primary cilia and intraflagellar transport proteins in the skeleton. Ann N Y Acad Sci. 2015;1335:78–99.
7. Miller KA, Ah-Cann CJ, Welfare MF, Tan TY, Pope K, Caruana G, Freckmann ML, Savarirayan R, Bertram JF, Dobbie MS, Bateman JF, Farlie PG. Cauli: a mouse strain with an Ift140 mutation that results in a skeletal ciliopathy modelling Jeune syndrome. PLoS Genet. 2013;9(8):e1003746.
8. Liem KF Jr, Ashe A, He M, Satir P, Moran J, Beier D, Wicking C, Anderson KV. The IFT-A complex regulates Shh signaling through cilia structure and membrane protein trafficking. J Cell Biol. 2012;197(6):789–800.

9. Fu W, Wang L, Kim S, Li J, Dynlacht BD. Role for the IFT-A complex in selective transport to the primary cilium. Cell Rep. 2016;17(6):1505–1517.
10. Duran I, Taylor SP, Zhang W, Martin J, Qureshi F, Jacques SM, Wallerstein R, Lachman RS, Nickerson DA, Bamshad M, Cohn DH, Krakow D. Mutations in IFT-A satellite core component genes IFT43 and IFT121 produce short rib polydactyly syndrome with distinctive campomelia. Cilia. 2017;6:7.
11. Bredrup C, Saunier S, Oud MM, Fiskerstrand T, Hoischen A, Brackman D, Leh SM, Midtbo M, Filhol E, Bole-Feysot C, Nitschke P, Gilissen C, Haugen OH, Sanders JS, Stolte-Dijkstra I, Mans DA, Steenbergen EJ, Hamel BC, Matignon M, Pfundt R, Jeanpierre C, Boman H, Rodahl E, Veltman JA, Knappskog PM, Knoers NV, Roepman R, Arts HH. Ciliopathies with skeletal anomalies and renal insufficiency due to mutations in the IFT-A gene WDR19. Am J Hum Genet. 2011;89(5):634–643.
12. Walczak-Sztulpa J, Eggenschwiler J, Osborn D, Brown DA, Emma F, Klingenberg C, Hennekam RC, Torre G, Garshasbi M, Tzschach A, Szczepanska M, Krawczynski M, Zachwieja J, Zwolinska D, Beales PL, Ropers HH, Latos-Bielenska A, Kuss AW. Cranioectodermal Dysplasia, Sensenbrenner syndrome, is a ciliopathy caused by mutations in the IFT122 gene. Am J Hum Genet. 2010;86(6):949–956.
13. Karsenty G. The complexities of skeletal biology. Nature. 2003;423(6937):316–318.
14. Arts HH, Bongers EM, Mans DA, van Beersum SE, Oud MM, Bolat E, Spruijt L, Cornelissen EA, Schuurs-Hoeijmakers JH, de Leeuw N, Cormier-Daire V, Brunner HG, Knoers NV, Roepman R. C14ORF179 encoding IFT43 is mutated in Sensenbrenner syndrome. J Med Genet. 2011;48(6):390–395.
15. Stokman MF, Oud MM, van Binsbergen E, Slaats GG, Nicolaou N, Renkema KY, Nijman IJ, Roepman R, Giles RH, Arts HH, Knoers NV, van Haelst MM. De novo 14q24.2q24.3 microdeletion including IFT43 is associated with intellectual disability, skeletal anomalies, cardiac anomalies, and myopia. Am J Med Genet A. 2016;170(6):1566–1569.
16. Huber C, Cormier-Daire V. Ciliary disorder of the skeleton. Am J Med Genet C Semin Med Genet. 2012;160C(3):165–174.
17. Perrault I, Saunier S, Hanein S, Filhol E, Bizet AA, Collins F, Salih MA, Gerber S, Delphin N, Bigot K, Orssaud C, Silva E, Baudouin V, Oud MM, Shannon N, Le Merrer M, Roche O, Pietrement C, Goumid J, Baumann C, Bole-Feysot C, Nitschke P, Zahrate M, Beales P, Arts HH, Munnich A, Kaplan J, Antignac C, Cormier-Daire V, Rozet JM. Mainzer-Saldino syndrome is a ciliopathy caused by IFT140 mutations. Am J Hum Genet. 2012;90(5):864–870.
18. Schmidts M, Frank V, Eisenberger T, Al Turki S, Bizet AA, Antony D, Rix S, Decker C, Bachmann N, Bald M, Vinke T, Toenshoff B, Di Donato N, Neuhann T, Hartley JL, Maher ER, Bogdanovic R, Peco-Antic A, Mache C, Hurles ME, Joksic I, Guc-Scekic M, Dobricic J, Brankovic-Magic M, Bolz HJ, Pazour GJ, Beales PL, Scambler PJ, Saunier S, Mitchison HM, Bergmann C. Combined NGS approaches identify mutations in the intraflagellar transport gene IFT140 in skeletal ciliopathies with early progressive kidney disease. Hum Mutat. 2013;34(5):714–724.
19. Pena-Padilla C, Marshall CR, Walker S, Scherer SW, Tavares-Macias G, Razo-Jimenez G, Bobadilla-Morales L, Acosta-Fernandez E, Corona-Rivera A, Mendoza-Londono R, Corona-Rivera JR. Compound heterozygous mutations in the IFT140 gene cause Opitz trigonocephaly C syndrome in a patient with typical features of a ciliopathy. Clin Genet. 2017;91(4):640–646.
20. Li G, Liu M, Zhang S, Wan H, Zhang Q, Yue R, Yan X, Wang X, Wang Z, Sun Y. Essential role of IFT140 in promoting dentinogenesis. J Dent Res. 2018;97(4):423–431.
21. Bouxsein ML, Boyd SK, Christiansen BA, Guldberg RE, Jepsen KJ, Muller R. Guidelines for assessment of bone microstructure in rodents using micro-computed tomography. J Bone Miner Res. 2010;25(7):1468–1486.
22. Ashe A, Butterfield NC, Town L, Courtney AD, Cooper AN, Ferguson C, Barry R, Olsson F, Liem KF Jr, Parton RG, Wainwright BJ, Anderson KV, Whitelaw E, Wicking C. Mutations in mouse Ift144 model the craniofacial, limb and rib defects in skeletal ciliopathies. Hum Mol Genet. 2012;21(8):1808–1823.
23. McInerney-Leo AM, Harris JE, Leo PJ, Marshall MS, Gardiner B, Kinning E, Leong HY, McKenzie F, Ong WP, Vodopiutz J, Wicking C, Brown MA, Zankl A, Duncan EL. Whole exome sequencing is an efficient, sensitive and specific method for determining the genetic cause of short-rib thoracic dystrophies. Clin Genet. 2015;88(6):550–557.
24. Pazour GJ, Dickert BL, Vucica Y, Seeley ES, Rosenbaum JL, Witman GB, Cole DG. ***Chlamydomonas*** IFT88 and its mouse homologue, polycystic kidney disease gene tg737, are required for assembly of cilia and flagella. J Cell Biol. 2000;151(3):709–718.
25. Moore ER, Yang Y, Jacobs CR. Primary cilia are necessary for Prx1-expressing cells to contribute to postnatal skeletogenesis. J Cell Sci. 2018;131(16):jcs217828.
26. Chang CF, Serra R. Ift88 regulates Hedgehog signaling, Sfrp5 expression, and beta-catenin activity in post-natal growth plate. J Orthop Res. 2013;31(3):350–356.
27. Yuan X, Cao J, He X, Serra R, Qu J, Cao X, Yang S. Ciliary IFT80 balances canonical versus non-canonical hedgehog signalling for osteoblast differentiation. Nat Commun. 2016;7:11024.
28. Helm BM, Willer JR, Sadeghpour A, Golzio C, Crouch E, Vergano SS, Katsanis N, Davis EE. Partial uniparental isodisomy of chromosome 16 unmasks a deleterious biallelic mutation in IFT140 that causes Mainzer-Saldino syndrome. Hum Genomics. 2017;11(1):16.
29. Chen J, Shi Y, Regan J, Karuppaiah K, Ornitz DM, Long F. Osx-Cre targets multiple cell types besides osteoblast lineage in postnatal mice. PLoS ONE. 2014;9(1):e85161.
30. Kronenberg HM. Developmental regulation of the growth plate. Nature. 2003;423(6937):332–336.